Theoretical Framework for Temporal Changes in Interactions among Adaptive Components of Living Systems

Ryunosuke Suzuki[1, 2, *] and Taiji Adachi[1, 2, 3, †]

[1] *Laboratory of Biomechanics, Department of Biosystems Science, Institute for Life and Medical Sciences, Kyoto University, 53 Shogoin-Kawahara-cho, Sakyo, Kyoto 606-8507, Japan*

[2] *Department of Micro Engineering, Graduate School of Engineering, Kyoto University, 53 Shogoin-Kawahara-cho, Sakyo, Kyoto 606-8507, Japan*

[3] *Department of Mammalian Regulatory Network, Graduate School of Biostudies, Kyoto University, 53 Shogoin-Kawahara-cho, Sakyo, Kyoto 606-8507, Japan*

(Dated: May 7, 2025)

In living systems, each component adaptively changes its internal states in response to its interactions with other components. These interactions, in turn, undergo temporal changes as a result of this adaptive behavior, which plays a crucial role in the emergence of system-level functions. Thus, to understand how changes in interactions influence the emergence of functions by employing models of adaptive behavior, it is essential to incorporate these interaction changes into these models. In this study, we developed a theoretical framework for modeling adaptive behavior of components under temporally changing interactions by formulating these interaction changes as dynamics of energy landscapes associated with that behavior. To represent this component-level adaptive behavior, internal state changes of each component were formulated based on the generalized gradient flow of an energy landscape and its associated energy rate landscape. We expressed dynamics of these landscapes by treating environmental states surrounding each component as temporal changes related to the interaction, which were then coupled to internal state changes of the component. Through case studies using simplified models of living systems under multiple mechanical interaction conditions among components, we demonstrated that our proposed theoretical framework can represent the emergence of functions of living systems. Even without explicitly defining adaptive behavior at the system level, these functions are specified based on the dynamics of the energy and energy rate landscapes of each component.

I. INTRODUCTION

Living systems, which consist of components such as molecules, cells, and tissues, exhibit functions that emerge from interactions among components as well as capabilities of individual living components. At the molecular scale, changes in biomolecular combinations [1, 2] and allosteric modulation of molecular interactions [3–5] regulate dynamics of molecular complexes. At the cellular scale, interactions between cells mediated by forces or biochemical signals regulate tissue dynamics such as morphogenesis [6, 7] and drive functional mechanisms such as suppression of tumor expansion [8, 9].

In response to interactions among these components, individual components in some living systems adaptively change their internal states, leading to the emergence of functions of an integrated living system as well as individual living components. For example, when living tissues interact mechanically, individual tissues grow or are remodeled in response, rendering their functional morphology as a system [10–12]. Moreover, temporal changes in interactions among living components affect functions of an integrated living system through adaptive behavior of individual components. For example, in the phenomenon known as the ball-and-socket ankle, which occurs in ankle joints during developmental processes, changes in the interactions among bones result in a shift from a typical hinge joint morphology to a spherical morphology [13]. This morphological change alters the functional range of motion of the joints [14]. Thus, interactions among living components play a crucial role in controlling the emergence of functions of an integrated living system through adaptive behavior of individual components.

A successful approach for characterizing adaptive behavior of living components is to build a theory based on energy landscapes. These energy landscapes symbolize the Waddington landscape, which reflects surrounding environment of living components [15, 16]. In this analogy, a position on the landscape corresponds to an adaptively changing internal state of a living component, whereas the adaptive behavior and temporal environment changes correspond to rolling of a ball and temporal landscape changes, respectively.

Previous studies have formulated adaptive behavior of living components using energy landscapes [17, 18]. Furthermore, by formulating an energy landscape of an integrated living system, a theory that incorporates system-level adaptation has revealed correspondence between a system-level energy landscape and individual landscapes of the components. Consequently, this theory has described temporal changes in individual energy landscapes

* Contact author: suzuki.ryunosuke.55s@st.kyoto-u.ac.jp
† Contact author: adachi@infront.kyoto-u.ac.jp

as landscape changes associated with system-level adaptation [19].

Adopting interactions among living components in energy landscape-based approaches is expected to capture the emergence of functions of an integrated living system controlled by these interactions. When considering interactions among living components, changes in surrounding environment of each component correspond to temporal interaction changes resulting from adaptive behavior of individual components. Therefore, to adopt interactions among components in these energy landscape-based approaches, it is necessary to formulate temporal changes in energy landscapes as a result of adaptive behavior of individual components rather than system-level adaptation. By developing such a framework, effects of temporal interaction changes due to adaptive behavior of individual components on the emergence of system functions can be discussed.

This study aims to propose a theoretical framework that embodies temporal changes in interactions among living components as those in their energy landscapes. By formulating adaptive internal state changes of individual living components and the resulting changes in their interactions, this framework embodies energy landscape changes for each living component. Additionally, through case studies using simplified models of living systems comprising mechanically interacting components, we demonstrate that the proposed framework enables discussions on effects of interaction changes due to adaptive behavior of individual components on the emergence of system functions.

II. THEORETICAL FRAMEWORK

In this chapter, to embody temporal changes in interactions among living components within a living system, we formulate adaptive behavior of individual living components and temporal changes in energy landscapes due to the adaptive behavior. First, we define graphs composed of component and interaction objects as shown in FIG. 1. Here, component objects (FIG. 1, squares) are introduced to describe adaptive behavior of individual living components and interaction objects (FIG. 1, circles) are introduced to describe temporal changes in interactions among components (FIG. 1). Next, we adopt the framework of the generalized gradient flow in the formulation of adaptive behavior of individual living components, given that it is well-suited for formulating internal state changes of living components viewed as dissipative behavior [19–21]. This framework assigns an energy function for each component object to define its energy landscape. Adaptive behavior of each component object are described by rolling of a ball in its energy landscape, where a position corresponds to an internal state of the component object. Furthermore, to describe temporal changes in energy functions of individual component objects due to their adaptive behavior, we formulate temporal environment changes surrounding each component object as functions of adaptive internal state changes of component objects connected through the same interaction object. These environment changes determine internal state changes of corresponding component objects. As a result, temporal changes in interactions among component objects, due to their adaptive behavior, are described as temporal changes in their energy landscapes.

A. Formulation of Adaptive Behavior of Individual Component Objects

To formulate adaptive behavior of individual component objects, for a solid square component object $i \in C$ in FIG. 1, where C is a set of component objects, $x_i(t) \in S_i^x$ denotes its internal states that adaptively change over time. To distinguish adaptively changing internal states from the other internal states, the non-adaptively changing internal states and total internal states are denoted as $y_i(t) \in S_i^y$ and $s_i(t)(= (x_i(t), y_i(t))) \in S_i(= S_i^x \times S_i^y)$, respectively. Here, S_i^x, S_i^y, and S_i are manifolds that form subspaces of Euclidean space. In contrast, open square component objects in FIG. 1 are assumed to behave non-adaptively, which is described as $s_i(t) = y_i(t)$. A rate of adaptive internal state of each component object are denoted as $\underline{\dot{x}}_i(t) \in T_x S_i^x$, which serve as a basis for determining an actual rate of internal state through temporal interaction changes among component objects. These rates are denoted as $\dot{x}_i(t) \in T_x S_i^x$, $\dot{y}_i(t) \in T_y S_i^y$, and $\dot{s}_i(t) \in T_s S_i$, where $T_x S_i^x$, $T_y S_i^y$, and $T_s S_i$ $(= T_x S_i^x \times T_y S_i^y)$ are the tangent spaces of S_i^x, S_i^y, and S_i, respectively. Note as $\underline{\dot{x}}_i(t) = 0$ is assumed for open square component objects because their internal states change non-adaptively over time.

For solid square component objects, which adaptively change their internal states, the rate $\underline{\dot{x}}_i(t) \in T_x S_i^x$ is formulated as dissipative behavior based on the framework of the generalized gradient flow [19, 21]. First, for a solid square component object $i \in C$, its energy function with the domain S_i^x is defined as

$$U_i[y_i(t)] : S_i^x \longrightarrow \mathbb{R};\ x_i \longmapsto U_i[y_i(t)](x_i), \tag{1}$$

where "$[y_i(t)]$" means that the energy function $U_i[y_i(t)]$ depends on the non-adaptively changing internal state $y_i(t)$, forming an energy landscape of the component object i (FIG. 2(a), blue curve).

Next, to formulate a rate of adaptive internal state of a component object as the generalized gradient flow of an energy landscape, energy change rate and energy dissipation rate functions of $\underline{\dot{x}}_i$ are defined as

$$J_i[s_i(t)] : T_x S_i^x \longrightarrow \mathbb{R};\ \underline{\dot{x}}_i \longmapsto \langle DU_i[y_i(t)](x_i(t)), \underline{\dot{x}}_i \rangle, \tag{2}$$

$$\Psi_i[s_i(t)] : T_x S_i^x \longrightarrow \mathbb{R};\ \underline{\dot{x}}_i \longmapsto \frac{1}{2}\langle \underline{\dot{x}}_i, \omega_i(s_i(t))\underline{\dot{x}}_i \rangle, \tag{3}$$

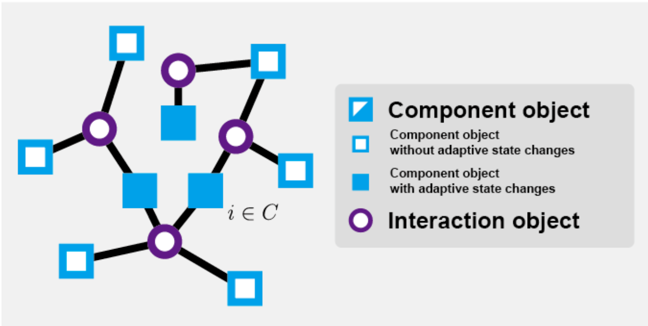

FIG. 1. Graph composed of component and interaction objects.

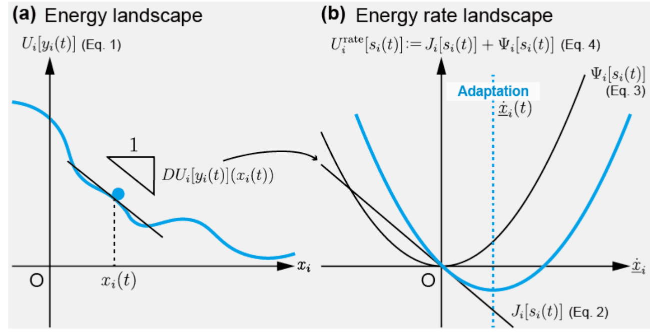

FIG. 2. Energy and energy rate landscapes of a component object $i \in C$. (a) Energy landscape formed by the energy function $U_i[y_i(t)]$. (b) Energy rate landscape formed by the function $U_i^{\text{rate}}[s_i(t)]$.

which are illustrated by a black line and parabola in FIG. 2(b). Here, when $T_x^* S_i^x$ denotes the cotangent space of the set of adaptively changing internal states S_i^x, $\langle \tau, \xi \rangle = \langle \xi, \tau \rangle \in \mathbb{R}$ is a contraction operation that returns a scalar quantity (an energy change rate in Eq. (2) or an energy dissipation rate in Eq. (3)) for $\tau \in T_x S_i^x$ and $\xi \in T_x^* S_i^x$. In addition, $DU_i[y_i(t)] : S_i^x \longrightarrow T_x^* S_i^x$ is a function that returns a derivative $DU_i[y_i(t)](x_i)$ of $U_i[y_i(t)]$ at x_i (FIG. 2(a), gradient of the black tangent line) for a given input x_i. Furthermore, the function $\omega_i : S_i \longrightarrow T_x^* S_i^x \times T_x^* S_i^x$ is a function of a total internal state $s_i(t)$ that provides the weight function $\omega_i(s_i(t)) : T_x S_i^x \longrightarrow T_x^* S_i^x$ that describes the energy dissipation rate for the adaptive behavior, ensuring that the energy dissipation rate function $\Psi_i[s_i(t)]$ is positive definite.

The sum of the energy change rate function $J_i[s_i(t)]$ and the energy dissipation rate function $\Psi_i[s_i(t)]$, that is, the net energy change rate function accounting for energy dissipation is defined as

$$U_i^{\text{rate}}[s_i(t)] := J_i[s_i(t)] + \Psi_i[s_i(t)] \tag{4}$$

which is illustrated by a blue parabola in FIG. 2(b), defining the condition for the temporal rate $\underline{\dot{x}}_i(t)$ of the adaptive internal state changes to be the generalized gradient flow as a minimization condition

$$\underline{\dot{x}}_i(t) \text{ minimizes } U_i^{\text{rate}}[s_i(t)]. \tag{5}$$

Thus, the function $U_i^{\text{rate}}[s_i(t)]$ forms an energy rate landscape for the component object i (FIG. 2(b), blue parabola), whose bottom determines temporal change rate $\underline{\dot{x}}_i(t)$ of the adaptive internal state changes (FIG. 2(b), blue dotted line). The temporal interaction changes convert this rate into the actual rate $\dot{x}_i(t)$, which in turn allows the internal state $x_i(t)$ to evolve within the energy landscape.

B. Formulation of Interaction Change among Component Objects

To formulate temporal interactions changes among component objects due to their adaptive behavior, let I denote a set of interaction objects, $\mathcal{V}_i^I \subset I$ a set of interaction objects adjacent to a component object $i \in C$, and $\mathcal{V}_j^C \subset C$ a set of component objects adjacent to an interaction object $j \in I$. With these objects, a situation in which component objects i and k are connected through the same interaction object j is expressed as $j \in \mathcal{V}_i^I$, $k \in \mathcal{V}_j^C$ (FIG. 3(a)). For an interaction object $j \in I$ and a component object $k \in \mathcal{V}_j^C$ (including the component object i), $S_{(k;j)}^z$ denotes a manifold that forms a subspace of Euclidean space, and its component $z_{(k;j)}(t) \in S_{(k;j)}^z$ denotes environmental states of the component object k associated with the interaction object j at time t.

To formulate temporal environment changes of a component object i due to adaptive behavior of individual component objects, we introduce a function $f_{(i;j)}$ ($j \in \mathcal{V}_i^I$), which maps a total internal state $s_k(t)$, a rate of adaptive internal state $\underline{\dot{x}}_k(t)$, and an environmental state $z_{(k;j)}(t)$, where $k \in \mathcal{V}_j^C$, to a temporal rate of environmental state $\dot{z}_{(i;j)}(t)$ of a component object i, denoted as

$$\begin{aligned} f_{(i;j)} : \prod_{k \in \mathcal{V}_j^C} (S_k \times T_x S_k^x \times S_{(k;j)}^z) &\longrightarrow T_z S_{(i;j)}^z; \\ (s_k(t), \underline{\dot{x}}_k(t), z_{(k;j)}(t))_{k \in \mathcal{V}_j^C} &\longmapsto \dot{z}_{(i;j)}(t) \end{aligned} \tag{6}$$

(FIG. 3(b)). Furthermore, to formulate actual internal state changes of a component object $i \in C$ due to changes in its environmental state, we introduce a function g_i, which maps the total internal state $s_i(t)$, the rate of adaptive internal state $\underline{\dot{x}}_i(t)$, and the environmental state $z_{(i;j)}(t)$ as well as its temporal rate $\dot{z}_{(i;j)}(t)$, where $j \in \mathcal{V}_i^I$, to a temporal rate of the internal state $\dot{s}_i(t)$, denoted as

$$g_i : S_i \times T_x S_i^x \times \prod_{j \in \mathcal{V}_i^I} \left(S_{(i;j)}^z \times T_z S_{(i;j)}^z \right) \longrightarrow T_s S_i (= T_x S_i^x \times T_y S_i^y);$$
$$\left(s_i(t), \underline{\dot{x}}_i(t), z_{(i;j)}(t), \dot{z}_{(i;j)}(t) \right)_{j \in \mathcal{V}_i^I} \longmapsto \dot{s}_i(t) (= (\dot{x}_i(t), \dot{y}_i(t))) \tag{7}$$

(FIG. 3(b)). Thus, the internal state changes of the component objects lead to the temporal changes in the adaptively changing internal state $x_i(t)$, the energy landscape formed by $U_i[y_i(t)]$, and the energy rate landscape formed by $U_i^{\mathrm{rate}}[s_i(t)]$ (FIG. 3(c), purple arrow).

Consequently, in addition to adaptive behavior of individual component objects, environmental and internal state changes ($\dot{z}_{(i;j)}(t)$ and $\dot{s}_i(t)$), each corresponding to adaptive internal state changes ($\underline{\dot{x}}_k(t)$), were formulated. Thus, this theoretical framework embodies temporal interaction changes among living components due to adaptive behavior of individual living components as energy landscape changes in response to a rate $\dot{y}_i(t)$ and energy rate landscape changes in response to a rate $\dot{s}_i(t)$.

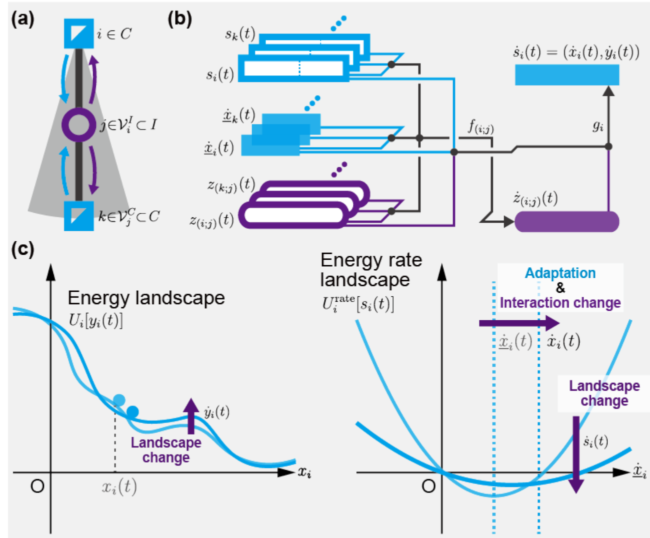

FIG. 3. Formulation of interaction among component objects. (a) Adjacency of a component object $i \in C$ and an interaction object $j \in I$. (b) Functions $f_{(i;j)}$ to formulate environmental state changes and g_i to formulate internal state changes. (c) Landscape changes caused by interaction changes due to adaptive internal state changes.

III. CASE STUDY

In this chapter, we show that our formulation of the temporal interaction changes among living components, induced by the adaptive behavior of individual components, as temporal changes in the energy and energy rate landscapes respectively formed by the functions $U_i[y_i(t)]$ and $U_i^{\mathrm{rate}}[s_i(t)]$ allows us to discuss the influence of these interaction changes among components on the emergence of functions of living systems without explicitly defining the adaptive behavior of integrated living systems. To achieve this, we define three different conditions for the functions $f_{(i;j)}$ and g_i ($i \in C, j \in \mathcal{V}_i^I$), which represent interactions among component objects, and examine how temporal changes in component interactions affect the emergence of functions under each condition of integrated living systems.

The first interaction condition (**GA**: Global adaptive interaction) explicitly defines the adaptive behavior of integrated living systems, which is associated with the functions $f_{(i;j)}$ and g_i. In contrast, instead of the adaptive behavior of the integrated living systems, the second (**EM**: energy landscape modified interaction) and third (**ErM**: energy rate landscape modified interaction) interaction conditions define the functions $f_{(i;j)}$ and g_i such that the temporal changes in the energy landscape and the energy rate landscape exhibit the emergence of functions of the system, respectively. By comparing the dynamics of the energy landscape between **GA** and **EM**, as well as the dynamics of the energy rate landscape between **GA** and **ErM**, we demonstrate that our theory can discuss the influence of the temporal changes in interactions on the emergence of functions of the integrated living system even when the interaction conditions do not explicitly define adaptive behavior of the systems.

A. Set Up of Adaptive State Changes of Living Components

In this section, we define internal and environmental states of component objects that constitute a system and adaptive internal state changes of individual component objects in response to their interactions. As an example of adaptive behavior, these case studies considers a scenario where individual living tissues undergo morphological changes in response to their mechanical interactions. For simplicity, we limit the number of component and interaction objects to two and one, denoted as $C = \{1, 2\}$ and $I = \{0\}$, respectively.

We model the component objects 1 and 2 constituting the system as rod-shaped living elements that adaptively change their cross-sectional areas $a_i(t)$ ($i = 1, 2$) in response to forces (FIG. 4(a)). Each component object i ($i = 1, 2$) is a linearly elastic rod with a constant natural length l_i and Young modulus e_i. These rods are connected in series at their respective natural lengths, with both ends fixed to rigid walls separated by a distance $l := l_1 + l_2$.

Each component object has its cross-sectional area $a_i(t)$ ($i = 1, 2$) as an adaptively changing internal state $x_i(t)$, denoted as

$$x_i(t) = a_i(t) \in S_i^x = \mathbb{R}_+, \tag{8}$$

where $\mathbb{R}_+(\subset \mathbb{R})$ represents the set of positive real numbers. Additionally, each component object has an internal state $y_i(t)$ that does not change over time due to adaptive behavior. This state consists of the axial strain $\epsilon_i(t)$, its gradient with respect to the cross-sectional area $\partial\epsilon_i/\partial a_i(t)$, and the weight $\omega_i(t)(:= \omega_i(s_i(t)))$ of the energy dissipation rate in adaptive behavior, denoted as

$$y_i(t) = \left(\epsilon_i(t), \frac{\partial \epsilon_i}{\partial a_i}(t), \omega_i(t)\right) \in S_i^y = \mathbb{R}^2 \times \mathbb{R}_+. \quad (9)$$

Consequently, a total internal state $s_i(t)$ of the component object i at time t is given by

$$s_i(t) = (x_i(t), y_i(t)) = \left(a_i(t), \epsilon_i(t), \frac{\partial \epsilon_i}{\partial a_i}(t), \omega_i(t)\right) \in S_i(= S_i^x \times S_i^y) = \mathbb{R}_+ \times \mathbb{R}^2 \times \mathbb{R}_+. \quad (10)$$

The connection between the component objects is under an external force p in their axial direction, as shown in FIG. 4(a). As a result of the mechanical interaction mediated by interaction object 0, each component object experiences a reaction force $r_i(t)$ $(i = 1, 2)$ from the rigid walls. Here, under the positive direction of the external and reaction forces p and $r_i(t)$ respectively defined as pointing from the component object 2 toward the component object 1 and from the wall toward the component object i, the equilibrium condition among these forces is given by $r_1(t) - r_2(t) + p = 0$. Additionally, the compatibility condition for the elastic deformation in the axial direction at the connection, expressed as $r_1(t)/(e_1a_1(t)/l_1)+r_2(t)/(e_2a_2(t)/l_2) = 0$. Consequently, the reaction force $r_i(t)$ and its gradient with respect to the cross-sectional area $\partial r_i/\partial a_i(t)$ are given by

$$r_i(t) := (-1)^i \frac{e_i a_i(t)/l_i}{\sum_{k\in C}(e_k a_k(t)/l_k)}\, p, \quad (11)$$

$$\frac{\partial r_i}{\partial a_i}(t) := (-1)^i \frac{(e_i/l_i)(e_j a_j(t)/l_j)}{\left(\sum_{k\in C}(e_k a_k(t)/l_k)\right)^2}\, p \quad (j \neq i). \quad (12)$$

To define temporal changes in strain $\epsilon_i(t)$ (where tensile strain is considered positive) and its gradient $\partial\epsilon_i/\partial a_i(t)$, which are influenced by the interaction changes (Eqs. 6 and 7), the reaction force $r_i(t)$ and its gradient $\partial r_i/\partial a_i(t)$ are incorporated as elements of the environmental state $z_{(i;0)}(t)$ surrounding the component object i associated with the interaction object j. Additionally, to define the interaction conditions **EM** and **ErM**, the environmental state $z_{(i;0)}(t)$ includes the elastic strain energy and its gradient with respect to the cross-sectional area, denoted as

$$U_i^z(t) = \frac{1}{2}\frac{e_i a_i(t)/l_i}{\left(\sum_{k\in C}(e_k a_k(t)/l_k)\right)^2}\, p^2, \quad (13)$$

$$\frac{\partial U_i^z}{\partial a_i}(t) = \frac{1}{2}\frac{(e_i/l_i)(e_j a_j(t)/l_j - e_i a_i(t)/l_i)}{\left(\sum_{k\in C}(e_k a_k(t)/l_k)\right)^3}\, p^2 \quad (j \neq i), \quad (14)$$

expressed using the external force p. Thus, the environmental state $z_{(i;0)}(t)$ is defined as

$$z_{(i;0)}(t) = \left(r_i(t), \frac{\partial r_i}{\partial a_i}(t), \frac{\partial U_i^z}{\partial a_i}(t)\right) \in S_{(i;0)}^z = \mathbb{R}^3. \quad (15)$$

The energy function that forms the energy landscape of each component object is defined as the elastic strain energy expressed by its total internal state $s_i(t) = (x_i(t), y_i(t))$. Therefore, the energy function $U_i[y_i(t)]$ (Eq. 1) and the energy change rate function $J_i[s_i(t)]$ (Eq. 2) are defined based on the strain $\epsilon_i(t)$ and its gradient with respect to the cross-sectional area $\partial\epsilon_i/\partial a_i(t)$, denoted as

$$U_i[y_i(t)](x_i) = \frac{1}{2} e_i l_i \epsilon_i(t)^2 a_i, \quad (16)$$

$$J_i[s_i(t)](\underline{\dot{x}}_i) = \frac{\partial U_i}{\partial a_i}[y_i(t)](x_i(t))\underline{\dot{a}}_i = \left(\frac{1}{2} e_i l_i \epsilon_i(t)^2 + e_i l_i \epsilon_i(t) \frac{\partial \epsilon_i}{\partial a_i}(t) a_i(t)\right)\underline{\dot{a}}_i. \quad (17)$$

In addition, the energy dissipation rate function $\Psi_i[s_i(t)]$ (Eq. 3) is defined based on Eq. (8) as

$$\Psi_i[s_i(t)](\underline{\dot{x}}_i) = \frac{1}{2}\omega_i(t)\underline{\dot{a}}_i^2. \quad (18)$$

By using these definitions, the rate $\underline{\dot{a}}_i(t)$ of adaptive cross-sectional area changes is defined based on Eqs. (4) and (5) as

$$\underline{\dot{a}}_i(t) = -\frac{1}{\omega_i(t)}\frac{\partial U_i}{\partial a_i}[y_i(t)](x_i(t)). \quad (19)$$

Thus, each component object has capability of decreasing its elastic strain energy $U_i[y_i(t)](x_i)$ at the rate $U_i^{\mathrm{rate}}[s_i(t)](\underline{\dot{x}}_i(t))$ through the cross-sectional area change rate $\underline{\dot{x}}_i(t) = \underline{\dot{a}}_i(t)$ following the minimization condition of Eq. (5).

B. Set Up of Interaction among Living Components

Next, by defining the actual rate $\dot{x}_i(t)$ of the internal state $x_i(t)$ through temporal interaction changes among the component objects, the rate $\dot{y}_i(t)$ that induces the temporal changes in the energy landscape formed by the function $U_i[y_i(t)]$, and the rate in $s_i(t)$ that induces the temporal changes in the energy rate landscape formed by the function $U_i^{\mathrm{rate}}[s_i(t)]$, which are illustrated in FIG. 3(c), we set the functions $f_{(i;0)}$ and g_i $(i = 1, 2)$ (Eqs. 6 and 7) to represent temporal changes in interactions among component objects for each interaction condition.

First, for simplicity, we employ the same function $f_{(i;0)}$ across all interaction conditions (**GA**, **EM**, **ErM**). Thus, under all interaction conditions, the rate $\dot{z}_{(i;0)}(t)$ (Eq. 6) of the environmental state of component object i includes the rates of the reaction force $r_i(t)$ (Eq. 11), reaction force gradient $(\partial r_i/\partial a_i)(t)$ (Eq. 12), and the elastic strain energy gradient $\partial U_i^z/\partial a_i(t)$ (Eq. 14), each in response to the cross-sectional area rate in adaptive behavior $(\underline{\dot{a}}_1(t), \underline{\dot{a}}_2(t))$, respectively denoted as

$$\dot{r}_i(t) = -\frac{\sum_{k,m\in C,\ m\neq k}(r_m(t)e_k\underline{\dot{a}}_k(t)/l_k)}{\sum_{k\in C}(e_k a_k(t)/l_k)}\ p,$$

$$\left(\dot{\overline{\frac{\partial r_i}{\partial a_i}}}\right)(t) = \frac{e_i}{l_i}\frac{\sum_{k\in C}\left(r_k(t)e_j\underline{\dot{a}}_j(t)/l_j\right) + 2r_j(t)e_i\underline{\dot{a}}_i(t)/l_i(i)}{\left(\sum_{k\in C}(e_k a_k(t)/l_k)\right)^2}\ p \quad (j \neq i), \tag{20}$$

$$\left(\dot{\overline{\frac{\partial U_i^z}{\partial a_i}}}\right)(t) = (-1)^i\frac{e_i}{l_i}\frac{\sum_{k,m\in C,\ m\neq k}(r_k(t) + 2r_m(t)e_k\underline{\dot{a}}_k(t)/l_k)}{\left(\sum_{k\in C}(e_k a_k(t)/l_k)\right)^3}\ p^2. \tag{21}$$

Next, we define the function g_i for each interaction condition. For simplicity, we assume that the actual cross-sectional area rate $\dot{a}_i(t)$ through temporal changes in interactions is identical to the adaptive cross-sectional area rate $\underline{\dot{a}}_i(t)$ ($\dot{a}_i(t) = \underline{\dot{a}}_i(t)$, or equivalently, $\dot{x}_i(t) = \underline{\dot{x}}_i(t)$). Under this simplification, each interaction condition defines the temporal changes in the internal state $y_i(t) = (\epsilon_i(t), \partial\epsilon_i/\partial a_i(t), \omega_i(t))$ induced by the function g_i.

1. *GA: global Adaptive Interaction*

To define the function g_i $(i = 1, 2)$ under the interaction condition **GA**, we associate the adaptive behavior of the integrated living system with the function g_i (FIG. 4(b)). For simplicity, we assume that the weight $\omega_i(t)$ of the energy dissipation rate in adaptive behavior remains constant, that is, $\dot{\omega}_i(t) = 0$. An energy function representing the elastic strain energy stored in the integrated system under the external force p, energy change rate function, energy dissipation rate function, and net energy change rate function are respectively defined as

$$U_0[y_1(t), y_2(t)](x_1, x_2) = \frac{1}{2}\frac{p^2}{\sum_{k\in C}(e_k a_k(t)/l_k)}, \tag{22}$$

$$J_0[s_1(t), s_2(t)](\underline{\dot{x}}_1, \underline{\dot{x}}_2) = \sum_{k\in C}\frac{\partial U_0}{\partial a_k}[y_1(t), y_2(t)](x_1(t), x_2(t))\underline{\dot{a}}_k, \tag{23}$$

$$\Psi_0[s_1(t), s_2(t)](\underline{\dot{x}}_1, \underline{\dot{x}}_2) = \sum_{k\in C}\Psi_k[s_k(t)](\underline{\dot{x}}_i), \tag{24}$$

$$U_0^{\mathrm{rate}}[s_1(t), s_2(t)](\underline{\dot{x}}_1, \underline{\dot{x}}_2) = (J_0[s_1(t), s_2(t)] + \Psi_0[s_1(t), s_2(t)])(\underline{\dot{x}}_1, \underline{\dot{x}}_2). \tag{25}$$

The cross-sectional area rates $(\underline{\dot{a}}_1(t), \underline{\dot{a}}_2(t))(= (\dot{a}_1(t), \dot{a}_2(t)))$ are assumed to satisfy the generalized gradient flow condition based on the function $U_0^{\mathrm{rate}}[s_1(t), s_2(t)]$, denoted as

$$(\underline{\dot{a}}_1(t), \underline{\dot{a}}_2(t)) \text{ minimizes } U_0^{\mathrm{rate}}[s_1(t), s_2(t)]. \tag{26}$$

For the cross-sectional area rate $\underline{\dot{a}}_i(t)$ of each component object i to simultaneously satisfy the generalized gradient flow condition based on the function $U_i^{\mathrm{rate}}[s_i(t)]$, this condition requires that the reaction force $r_i(t)$ among its environmental states be reflected in its internal state whereas the reaction force gradient $\partial r_i/\partial a_i(t)$ not be. Consequently, the strain $\epsilon_i(t)$ and its gradient with respect to the cross-sectional area $\partial\epsilon_i/\partial a_i(t)$ are given by

$$\epsilon_i(t) = -\frac{r_i(t)}{e_i a_i(t)}, \tag{27}$$

$$\frac{\partial\epsilon_i}{\partial a_i}(t) = \frac{r_i(t)}{e_i a_i(t)^2}. \tag{28}$$

Thus, under the interaction condition **GA**, which satisfies these equations, the strain rate and strain gradient rate of component object i, defined by the function g_i are derived as

$$\dot{\epsilon}_i(t) = -\frac{\dot{r}_i(t)a_i(t) - r_i(t)\underline{\dot{a}}_i(t)}{e_i a_i(t)^2}, \tag{29}$$

$$\left(\dot{\overline{\frac{\partial\epsilon_i}{\partial a_i}}}\right)(t) = \frac{\dot{r}_i(t)a_i(t) - 2r_i(t)\underline{\dot{a}}_i(t)}{e_i a_i(t)^3}. \tag{30}$$

2. *EM: energy Landscape Modified Interaction*

The interaction condition **EM** defines function g_i so that temporal changes in the energy landscape, instead of the adaptive behavior of the integrated living system, specify the emergence of a function of the integrated living system (FIG. 4(c)). In **EM**, not only the reaction force $r_i(t)$, but also its gradient $\partial r_i/\partial a_i(t)$ is reflected in the internal state of each component object. Accordingly, the strain gradient $\partial\epsilon_i/\partial a_i(t)$ and its rate $(\dot{\overline{\partial\epsilon_i/\partial a_i}})(t)$

are respectively modified from Eqs. (28) and (30) to

$$\frac{\partial \epsilon_i}{\partial a_i}(t) = \frac{r_i(t)}{e_i a_i(t)^2} - \frac{\partial r_i/\partial a_i(t)}{e_i a_i(t)}, \tag{31}$$

$$\left(\dot{\overline{\frac{\partial \epsilon_i}{\partial a_i}}}\right)(t) = \frac{\dot{r}_i(t) a_i(t) - 2 r_i(t) \underline{\dot{a}}_i(t)}{e_i a_i(t)^3} - \frac{(\dot{\overline{\partial r_i/\partial a_i}})(t) a_i(t) - (\partial r_i/\partial a_i)(t) \underline{\dot{a}}_i(t)}{e_i a_i(t)^2} \tag{32}$$

(FIG. 4(c)). As a result, the energy gradient $\partial U_i/\partial a_i[y_i(t)](x_i(t))$ and its rate $(\dot{\overline{\partial U_i/\partial a_i}})(t)$ of each component object coincide with $\partial U_i^z/\partial a_i(t)$ (Eq. 14) and its rate $(\dot{\overline{\partial U_i^z/\partial a_i}})(t)$ (Eq. 21), respectively. Therefore, the signs of the cross-sectional area rate $\underline{\dot{a}}_i(t)$ (Eq. 19) and the energy gradient rate $(\dot{\overline{\partial U_i/\partial a_i}})(t)$ hold antisymmetry between the component objects, respectively expressed as

$$\sum_{k \in C} \left(\frac{\omega_k(0)}{e_k/l_k} \underline{\dot{a}}_k(t) \right) = \sum_{k \in C} \left(-\frac{l_k}{e_k} \frac{\partial U_k}{\partial a_k}[y_k(t)](x_k(t)) \right) = 0, \tag{33}$$

$$\sum_{k \in C} \left(\frac{\omega_k(0)}{e_k/l_k} \underline{\ddot{a}}_k(t) \right) = \sum_{k \in C} \left(-\frac{l_k}{e_k} \left(\dot{\overline{\frac{\partial U_k}{\partial a_k}}} \right)(t) \right) = 0. \tag{34}$$

Thus, under the interaction condition **EM**, the integrated living system exhibits a function that makes the symmetry between the signs of the cross-sectional area rate $\dot{a}_i(t) (= \underline{\dot{a}}_i(t))$ and its acceleration $\ddot{a}_i(t) (= \underline{\ddot{a}}_i(t))$ consistent across the component objects.

3. *ErM: energy Rate Landscape Modified Interaction*

The interaction condition **ErM** defines function g_i so that temporal changes in the energy rate landscape, instead of the adaptive behavior of the integrated living system, specify the emergence of a function of the integrated living system (FIG. 4(d)). In **ErM**, in addition to the strain gradient rate $(\dot{\overline{\partial \epsilon_i/\partial a_i}})(t)$, the rate of the weight $\omega_i(t)$ of the energy dissipation rate is modified from $\dot{\omega}_i(t) = 0$ to be dependent on the elastic strain energy gradient rate $(\dot{\overline{\partial U_i^z/\partial a_i}})(t)$, expressed as

$$\dot{\omega}_i(t) = \omega_i(t) \frac{(\dot{\overline{\partial U_i^z/\partial a_i}})(t)}{\partial U_i^z/\partial a_i(t)}. \tag{35}$$

(FIG. 4(d)). Consequently, the cross-sectional area acceleration $\underline{\ddot{a}}_i(t)$ (Eq. 19) for each component object satisfies

$$\underline{\ddot{a}}_i(t) = \frac{1}{\omega_i(t)^2} \left(\dot{\omega}_i(t) \frac{\partial U_i^z}{\partial a_i}(t) - \omega_i(t) \left(\dot{\overline{\frac{\partial U_i^z}{\partial a_i}}}(t) \right) \right) = 0. \tag{36}$$

Thus, under the interaction condition **ErM**, the integrated living system exhibits a function that stabilizes the cross-sectional area rate $\underline{\dot{a}}_i(t)$ of each component object.

C. Results

Under each interaction condition (**GA**, **EM**, **ErM**) defined in the previous section, we analyzed the behavior of the cross-sectional areas, as well as the energy or energy rate landscape of each component over time (FIG. 5, 6). Here, the time interval for analyzing the system dynamics was defined as $t \in [0, T]$ by using a constant T. For simplicity, the initial values of the cross-sectional area $a_i(0)$ and Young modulus e_i were consistent across the components, given by $a_i(0) = a$ (= const.) and $e_i = e$ (= const.), respectively. To make the initial cross-sectional area rates $\dot{a}_i(0)$ nonzero under **EM**, the natural lengths l_i are set as $l_1 = 0.6\ l$, $l_2 = 0.4\ l$ by using the constant l $(= l_1 + l_2)$, which represents the distance between the rigid walls. Additionally, the initial weight $\omega_i(0)$ of the energy dissipation rate in adaptive behavior was consistent across the components, given by $\omega_i(0) = \bar{\omega} l_i^2$ by using a constant $\bar{\omega}$ and the length l_i.

In FIG. 5, to confirm the emergence of the function of the integrated living system under the interaction condition **EM** through the energy landscape dynamics of the component objects, we illustrate the dynamics of the cross-sectional area $a_i(t)$, the energy $U_i[y_i(t)](x_i(t))$, and the energy landscape formed by the energy function $U_i[y_i(t)]$ under the interaction conditions **GA** and **EM** in FIG. 5(a) and (b), respectively. Here, the cross-sectional area $a_i(t)$ and the energy $U_i[y_i(t)](x_i(t))$ were normalized by using their initial values, $a_i(0) = a$ and $U_i[y_i(0)](x_i(0))$.

Under the interaction condition **GA**, because the energy gradient $\partial U_i/\partial a_i[y_i(t)](x_i(t))$ (Eq. 17) under substitution of the strain $\epsilon_i(t)$ (Eq. 27) and its gradient $\partial \epsilon_i/\partial a_i(t)$ (Eq. 28) is always positive, as illustrated by the trajectories of the points (blue arrow) in FIG. 5(a), the cross-sectional areas $a_i(t)$ of both component objects increased over time. For component object 1, in response to the interaction changes, the energy landscape formed by the energy function $U_1[y_1(t)]$ (Eq. 16) sank over time, as illustrated by the trajectory of the curve (purple arrow) in FIG. 5(a). Consequently, due to the effects of cross-sectional area increase and landscape sinking, the energy $U_1[y_1(t)](x_1(t))$ decreased. On the other hand, for component object 2, although the energy landscape rose, the effect of the increasing cross-sectional area outweighed the effect of the landscape rising. As a result, similar to component object 1, the energy $U_2[y_2(t)](x_2(t))$ decreased.

Under the interaction condition **EM**, as illustrated by the trajectory of the points (blue line) in FIG. 5(b), the cross-sectional area rate $\dot{a}_1(t)$ of component object 1 turned into negative. Furthermore, as illustrated by the

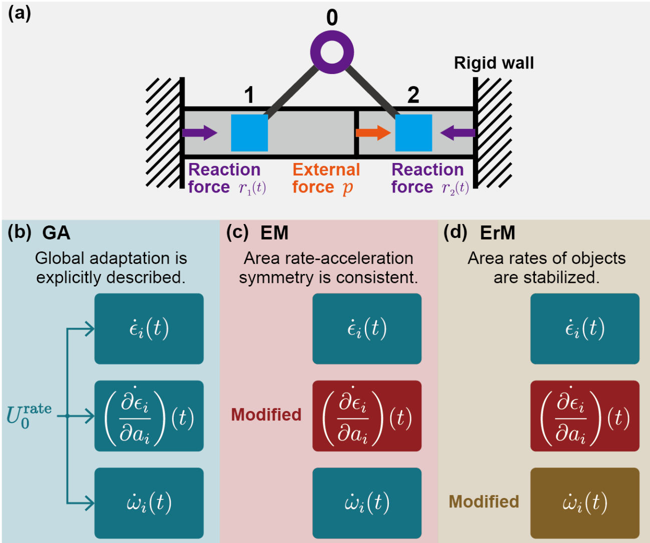

FIG. 4. Set up of the case studies. (a) System considered in the case studies: the component objects 1 and 2 correspond to living components that behave as elastic bars and mechanically interact via the interaction object 0 under the external force p at their joint; each component object experiences the reaction force $r_i(t)$ at the fixed point on the rigid wall. (b) Interaction condition **GA**: global adaptive interaction. (c) Interaction condition **EM**: energy landscape modified interaction. (d) Interaction condition **ErM**: energy rate landscape modified interaction.

trajectory of the landscape (purple curve) in FIG. 5(b), the energy gradient $\partial U_1/\partial a_1[y_1(t)](x_1(t))$ decreased due to the landscape changes, leading to a reduction in the cross-sectional area acceleration $\ddot{a}_1(t)$ of component object 1. On the other hand, for component object 2, due to the antisymmetric relationship of the signs of the cross-sectional area rates $\dot{a}_i(t)$ $(i = 1, 2)$ between objects (Eq. 33), the cross-sectional area rate $\dot{a}_2(t)$ increased. Furthermore, because the sign of the energy gradient rate $\dot{(\partial U_i/\partial a_i)}(t)$ is also antisymmetric between objects (Eq. 34), the energy gradient $\partial U_2/\partial a_2[y_2(t)](x_2(t))$ increased with the landscape change, leading to an increase in the cross-sectional area acceleration $\ddot{a}_2(t)$ of component object 2. Thus, under the interaction condition **EM**, the function that makes the symmetry between the sign of the cross-sectional area rate $\dot{a}_i(t)$ and its acceleration $\ddot{a}_i(t)$ consistent across the component objects was confirmed through the energy landscape dynamics of the component objects.

In FIG. 6, to confirm the emergence of the function of the integrated living system under the interaction condition **ErM** through the energy rate landscape dynamics of the component objects, we illustrated the dynamics of the weight $\omega_i(t)$ of the energy dissipation rate in adaptive behavior and the cross-sectional area rate $\dot{a}_i(t)$ under the interaction conditions **GA** and **ErM** in FIG. 6(a) and (b), respectively. Here, the time t was normalized by using the constant T. Additionally, the weight $\omega_i(t)$ of the energy dissipation rate and the cross-sectional area rate $\dot{a}_i(t)$ are normalized by using their respective initial values $\omega_i(0) = \bar{\omega} l_i^2$ and $\dot{a}_i(0)$, respectively.

Under the interaction condition **GA**, as shown in FIG. 6(a), the weight $\omega_i(t)$, that is, the slope of the energy rate landscape remained constant since the rate $\dot{\omega}_i(t)$ of the weight was set to be constant. Additionally, since the energy gradient $-\partial U_i/\partial a_i[y_i(t)](x_i(t))$ decreased as the cross-sectional area increased, the cross-sectional area rate $\dot{a}_i(t) = -\omega_i(t)^{-1}\partial U_i/\partial a_i[y_i(t)](x_i(t))$ decreased over time.

Under the interaction condition **ErM**, as the rate of the weight $\omega_i(t)$ was variable according to Eq. (35), the slope of the energy rate landscape changed over time, as shown in FIG. 6(b). As a result, as derived from Eq. (36), the cross-sectional area rate $\dot{a}_i(t)$ of each component object remained constant. Thus, under the interaction condition **ErM**, the function that stabilizes the cross-sectional area rate $\dot{a}_i(t)$ of each component object was confirmed through the energy rate landscape dynamics of each component object.

Through the above case studies under three interaction conditions, the influence of temporal interaction changes on the emergence of functions of integrated living systems was demonstrated to be discussed by specifying the function of the integrated living system based on the dynamics of the energy landscapes and energy rate landscapes of individual component objects, not only under interaction conditions where the adaptive behavior of the integrated living system is explicitly defined (such as interaction condition **GA** in the case studies) but also under interaction conditions where it is not (such as interaction conditions **EM** and **ErM** in the case studies).

IV. DISCUSSION

In this study, focusing on living systems composed of interacting living components, we developed a theoretical framework that embodies temporal interaction changes, which are driven by the adaptive behavior of individual living components, based on temporal changes in energy landscapes. For the adaptive behavior of individual living components constituting a living system, we provided a formulation according to the generalized gradient flow of an energy landscape. Moreover, as interaction changes among component objects induced by their adaptive behavior, we formulated temporal changes in the environmental state $z_{(k;j)}(t)$ $(j \in \mathcal{V}_i^I,\ k \in \mathcal{V}_j^C)$ surrounding each component object and in the total internal state $s_i(t) = (x_i(t), y_i(t))$ of each component object, each in response to the rate of adaptive internal state changes $\dot{\underline{x}}_i(t)$. Through this sequential formulation, interaction changes among component objects were represented as temporal changes in the energy and energy rate landscapes respectively formed by the functions $U_i[y_i(t)]$ and $U_i^{\mathrm{rate}}[s_i(t)]$.

Through the case studies based on the proposed the-

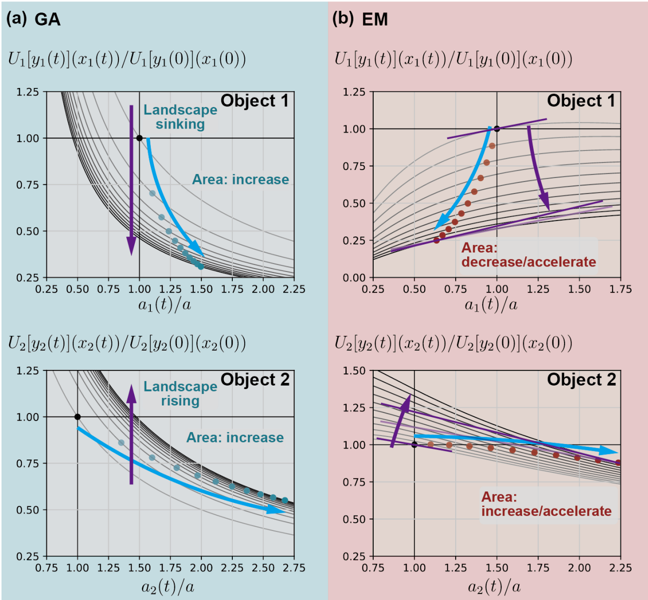

FIG. 5. Changes in the sectional areas, energies, and energy landscapes over time (a) under **GA**: global adaptive interaction, and (b) under **EM**: energy landscape modified interaction.

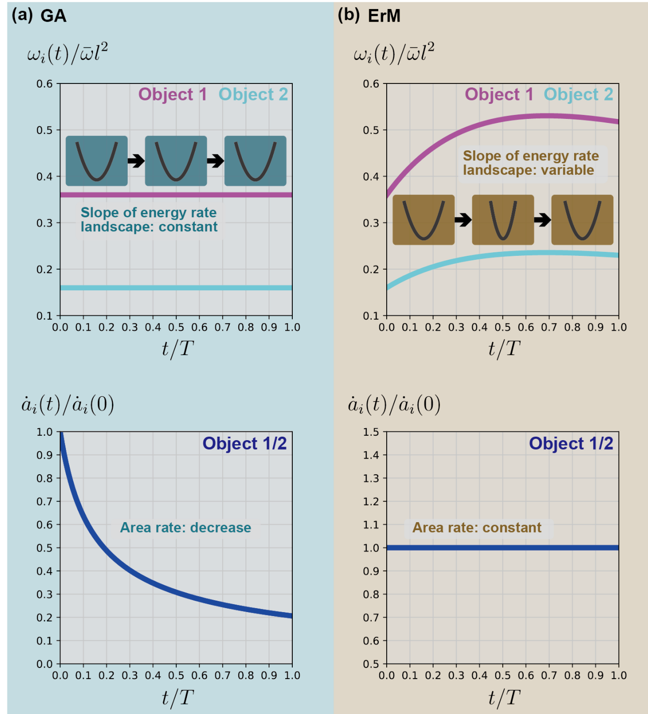

FIG. 6. Changes in the slopes of the energy rate landscapes and sectional area rates over time (a) under **GA**: global adaptive interaction, and (b) under **ErM**: energy rate landscape modified interaction.

ory, we demonstrated that, under an interaction condition that explicitly sets the adaptive behavior of the integrated living system according to the function $U_0[y_1(t), y_2(t)](x_1, x_2)$ (**GA**), the energy landscape-based representation of temporal interaction changes allowed us to associate the interaction changes with the emergence of the function of the integrated living system. Furthermore, even under the interaction conditions without explicitly setting adaptive behavior of the integrated living system (**EM**, **ErM**), setting the temporal changes in the energy and energy rate landscapes could represent the emergence of the functions of the integrated living system resulting from the interaction changes. Therefore, it was confirmed possible to discuss the influence of interaction changes on the emergence of functions of integrated living systems by specifying a function through the dynamics of the energy and energy rate landscapes of individual component objects, regardless of whether interaction conditions explicitly define the adaptive behavior of integrated living systems.

In this study, we conceptualized changes in the surrounding environment of each living component as temporal interaction changes among components driven by their adaptive behavior and formulated these interaction changes as temporal changes in energy and energy rate landscapes. Applying this landscape-based theoretical approach to actual living phenomena would contribute to understanding the mechanisms underlying the emergence of functions of integrated living systems where the environment of each component temporally changes along with interactions among components. Examples of dynamically changing environment under component interactions include the microenvironment reconstructed during epithelial-mesenchymal transition [22], the tumor microenvironment formed through signal exchange between cancer and non-cancerous cells [23], and the inflammatory or regenerative microenvironment shaped by the molecular secretion of senescent cells (senescence-associated secretory phenotype) [24, 25]. By applying our theoretical framework to these environment, diverse living phenomena would be understood from a unified perspective based on the adaptive behavior of individual living components and the resulting temporal changes in their interactions.

Furthermore, not only living systems but also artificial systems such as swarm robots [26] and soft robots [27, 28], which exhibit behavior inspired by living systems, can benefit from our theoretical framework for modeling interactions among components. When designing these artificial systems, considering only the behavior of individual components may require a detailed design of the behavior of each component over time to align with an intended system-wide behavior. By applying our theoretical framework to artificial system design, instead of increasing the complexity of designing individual component behavior, it can become possible to design temporal changes in interactions among components in response to their adaptive behavior. Consequently, this approach is expected to enable the emergence of integrated system functions while maintaining simple design requirements for individual components.

In this study, we assumed that each component object corresponds to a single living component, and thus, the interaction objects did not support interactions at the level of clusters composed of multiple living components. To overcome this limitation, incorporating hypergraph theory could be an effective approach. In a hypergraph, hyperedges are defined as subsets of a node set, and thus, each hyperedge can be interpreted as a cluster of nodes. Therefore, introducing a hypergraph where each node corresponds to a living component and assigning hyperedges to component objects would allow a single component object to treat clusters of living components. This approach enables, for example, both the energy landscapes respectively representing the adaptive behavior of an individual living component and of a cluster containing that component to change in response to interaction changes, and consequently, this extension allows for more flexible and appropriate modeling of living system dynamics.

Furthermore, mathematical refinements represented by the above extensions would facilitate the integration of this theoretical framework with other theories that focus on interactions among living components and enable a broader mathematical perspective for understanding how temporal changes in interactions influence the emergence of functions of integrated living systems. To describe living system dynamics under component interactions, various theories have been proposed based on, for example, the Hopfield network [29], the information thermodynamics [2], and the game theory [30]. Applying our theoretical framework to these existing theories, which are available for modeling living systems, could enable these theories to explicitly describe the effects of temporal changes in interactions, which have thus far only been considered implicitly, by using temporal changes in energy and energy rate landscapes.

ACKNOWLEDGMENT

This work was supported by Grant-in-Aid for Scientific Research (A) (JP25H01219) and (A) (JP20H00659) from Japan Society for the Promotion of Science (JSPS); JST-CREST (JPMJCR22L5) and JST SPRING (JPMJSP2110) from Japan Science and Technology Agency (JST).

AUTHOR CONTRIBUTIONS

Ryunosuke Suzuki: Writing - review and editing, Writing - original draft, Visualization, Software, Resources, Methodology, Investigation, Funding acquisition, Formal analysis, Conceptualization. **Taiji Adachi**: Writing - review and editing, Supervision, Resources, Project administration, Funding acquisition, Conceptualization.

[1] I. Beusch and H. D. Madhani, Understanding the dynamic design of the spliceosome, Trends in Biochemical Sciences **49**, 583 (2024).

[2] S. Borsley, Membrane Transport, Molecular Machines, and Maxwell's Demon, ChemSystemsChem **6**, e202400004 (2024).

[3] S. J. Wodak, E. Paci, N. V. Dokholyan, I. N. Berezovsky, A. Horovitz, J. Li, V. J. Hilser, I. Bahar, J. Karanicolas, G. Stock, P. Hamm, R. H. Stote, J. Eberhardt, Y. Chebaro, A. Dejaegere, M. Cecchini, J.-P. Changeux, P. G. Bolhuis, J. Vreede, P. Faccioli, S. Orioli, R. Ravasio, L. Yan, C. Brito, M. Wyart, P. Gkeka, I. Rivalta, G. Palermo, J. A. McCammon, J. Panecka-Hofman, R. C. Wade, A. Di Pizio, M. Y. Niv, R. Nussinov, C.-J. Tsai, H. Jang, D. Padhorny, D. Kozakov, and T. McLeish, Allostery in Its Many Disguises: From Theory to Applications, Structure **27**, 566 (2019).

[4] H. Hofmann, All over or overall – Do we understand allostery?, Current Opinion in Structural Biology **83**, 102724 (2023).

[5] N. Wu, M. Barahona, and S. N. Yaliraki, Allosteric communication and signal transduction in proteins, Current Opinion in Structural Biology **84**, 102737 (2024).

[6] H. Vignes, C. Vagena-Pantoula, and J. Vermot, Mechanical control of tissue shape: Cell-extrinsic and -intrinsic mechanisms join forces to regulate morphogenesis, Seminars in Cell & Developmental Biology **130**, 45 (2022).

[7] J. Su, Y. Song, Z. Zhu, X. Huang, J. Fan, J. Qiao, and F. Mao, Cell–cell communication: new insights and clinical implications, Signal Transduction and Targeted Therapy **9**, 196 (2024).

[8] M. E. Van Luyk, A. Krotenberg Garcia, M. Lamprou, and S. J. E. Suijkerbuijk, Cell competition in primary and metastatic colorectal cancer, Oncogenesis **13**, 28 (2024).

[9] S. Kim, D. Lee, S. E. Kim, and M. Overholtzer, Entosis: the core mechanism and crosstalk with other cell death programs, Experimental & Molecular Medicine **56**, 870 (2024).

[10] N. Felsenthal and E. Zelzer, Mechanical regulation of musculoskeletal system development, Development **144**, 4271 (2017).

[11] D. Ambrosi, M. Ben Amar, C. J. Cyron, A. DeSimone, A. Goriely, J. D. Humphrey, and E. Kuhl, Growth and remodelling of living tissues: perspectives, challenges and opportunities, Journal of The Royal Society Interface **16**, 20190233 (2019).

[12] M. L. Killian, Growth and mechanobiology of the tendon-bone enthesis, Seminars in Cell & Developmental Biology **123**, 64 (2022).

[13] P. M. Stevens, S. Aoki, and P. Olson, Ball-and-Socket Ankle, Journal of Pediatric Orthopaedics **26**, 427 (2006).

[14] J. R. Jastifer, P. A. Gustafson, A. Labomascus, and T. Snoap, Ball and Socket Ankle: Mechanism and Computational Evidence of Concept, The Journal of Foot and Ankle Surgery **56**, 773 (2017).

[15] C. Waddington, *The Strategy of the Genes* (Routledge, London, 1957).

[16] C. H. Waddington, *The Nature of Life* (Routledge, London, 1961).

[17] C. Furusawa and K. Kaneko, A Dynamical-Systems View of Stem Cell Biology, Science **338**, 215 (2012).

[18] Y. Matsushita and K. Kaneko, Homeorhesis in Waddington's landscape by epigenetic feedback regulation, Physical Review Research **2**, 023083 (2020).

[19] S. A. Horiguchi and T. J. Kobayashi, Cellular gradient flow structure linking single-cell-level rules and population-level dynamics, Physical Review Research **5**, L022052 (2023).

[20] A. Mielke, A gradient structure for reaction–diffusion systems and for energy-drift-diffusion systems, Nonlinearity **24**, 1329 (2011).

[21] M. A. Peletier, Variational modelling: Energies, gradient flows, and large deviations (2014), arXiv:1402.1990.

[22] K. K. Youssef and M. A. Nieto, Epithelial–mesenchymal transition in tissue repair and degeneration, Nature Reviews Molecular Cell Biology **25**, 720 (2024).

[23] K. E. De Visser and J. A. Joyce, The evolving tumor microenvironment: From cancer initiation to metastatic outgrowth, Cancer Cell **41**, 374 (2023).

[24] D. Paramos-de Carvalho, A. Jacinto, and L. Saúde, The right time for senescence, eLife **10**, e72449 (2021).

[25] Y. Saito, S. Yamamoto, and T. S. Chikenji, Role of cellular senescence in inflammation and regeneration, Inflammation and Regeneration **44**, 28 (2024).

[26] L. Yang, J. Yu, S. Yang, B. Wang, B. J. Nelson, and L. Zhang, A Survey on Swarm Microrobotics, IEEE Transactions on Robotics **38**, 1531 (2022).

[27] R. Baines, F. Fish, J. Bongard, and R. Kramer-Bottiglio, Robots that evolve on demand, Nature Reviews Materials **9**, 822 (2024).

[28] L. C. Van Laake and J. T. B. Overvelde, Bio-inspired autonomy in soft robots, Communications Materials **5**, 198 (2024).

[29] L. Herron, P. Sartori, and B. Xue, Robust Retrieval of Dynamic Sequences through Interaction Modulation, PRX Life **1**, 023012 (2023).

[30] Y. Fujimoto and S. Ito, Game-theoretical approach to minimum entropy productions in information thermodynamics, Physical Review Research **6**, 013023 (2024).